



Intranasal administration of polysulfide prevents neurodegeneration in spinal cord and rescues mice from delayed paraplegia after spinal cord ischemia

Eiki Kanemaru^{a,1}, Yusuke Miyazaki^{a,1}, Eizo Marutani^a, Mariko Ezaka^a, Shunsaku Goto^a, Etsuo Ohshima^b, Donald B. Bloch^c, Fumito Ichinose^{a,*}

^a Anesthesia Center for Critical Care Research, Department of Anesthesia, Critical Care and Pain Medicine, Massachusetts General Hospital and Harvard Medical School, Boston, MA, 02114, USA

^b Corporate Strategy Department, Kyowa Hakko Bio Co., Ltd., Tokyo, 164-0001, Japan

^c Department of Medicine, Division of Rheumatology, Allergy and Immunology, Massachusetts General Hospital, Boston, MA, 02114, USA

ARTICLE INFO

Keywords:

Delayed paraplegia
Glutathione trisulfide (GSSSG)
Hydrogen sulfide (H₂S)
Pantethine trisulfide (PTN-SSS)
Spinal cord ischemia
Sulfane sulfur (S⁰)

ABSTRACT

Background: Delayed paraplegia is a devastating complication of thoracoabdominal aortic surgery. Hydrogen sulfide (H₂S) was reported to be protective in a mouse model of spinal cord ischemia and the beneficial effect of H₂S has been attributed to polysulfides. The objective of this study was to investigate the effects of polysulfides on delayed paraplegia after spinal cord ischemia.

Methods and results: Spinal cord ischemia was induced in male and female C57BL/6J mice by clamping the aortic arch and the left subclavian artery. Glutathione trisulfide (GSSSG), glutathione (GSH), glutathione disulfide (GSSG), or vehicle alone was administered intranasally at 0, 8, 23, and 32 h after surgery. All mice treated with vehicle alone developed paraplegia within 48 h after surgery. GSSSG, but not GSH or GSSG, prevented paraplegia in 8 of 11 male mice (73%) and 6 of 8 female mice (75%). Intranasal administration of ³⁴S-labeled GSSSG rapidly increased ³⁴S-labeled sulfane sulfur species in the lumbar spinal cord. In mice treated with intranasal GSSSG, there were increased sulfane sulfur levels, and decreased neurodegeneration, microglia activation, and caspase-3 activation in the lumbar spinal cord. In vitro studies using murine primary cortical neurons showed that GSSSG increased intracellular levels of sulfane sulfur. GSSSG, but not GSH or GSSG, dose-dependently improved cell viability after oxygen and glucose deprivation/reoxygenation (OGD/R). Pantethine trisulfide (PTN-SSS) also increased intracellular sulfane sulfur and improved cell viability after OGD/R. Intranasal administration of PTN-SSS, but not pantethine, prevented paraplegia in 6 of 9 male mice (66%).

Conclusions: Intranasal administration of polysulfides rescued mice from delayed paraplegia after transient spinal cord ischemia. The neuroprotective effects of GSSSG were associated with increased levels of polysulfides and sulfane sulfur in the lumbar spinal cord. Targeted delivery of sulfane sulfur by polysulfides may prove to be a novel approach to the treatment of neurodegenerative diseases.

1. Introduction

Approximately 2–12% of patients who undergo thoracoabdominal aortic surgery experience the devastating complication of paraplegia [1, 2]. More than 80% of the post-surgical paraplegia is reported to be

delayed and is caused by secondary neuronal injury in the spinal cord [3, 4]. Although the pathogenetic mechanism of secondary neuronal injury is incompletely understood, increased oxidative stress, mitochondrial dysfunction, inflammation, apoptosis, and glutamate-mediated excitotoxicity have been suggested to play key roles [5,6]. Because the

* Corresponding author. Anesthesia Center for Critical Care Research, Department of Anesthesia, Critical Care and Pain Medicine, Massachusetts General Hospital, Thier 503, 50 Blossom St, Boston, MA, 02114, USA.

E-mail addresses: ekanemaru@mgh.harvard.edu (E. Kanemaru), y.miyazaki@jikei.ac.jp (Y. Miyazaki), emarutani@mgh.harvard.edu (E. Marutani), mmarico04@yahoo.co.jp (M. Ezaka), sgoto2@mgh.harvard.edu (S. Goto), etsuo.ohshima@kyowa-kirin.co.jp (E. Ohshima), dbloch@mgh.harvard.edu (D.B. Bloch), fichinose@mgh.harvard.edu (F. Ichinose).

¹ Both authors contributed equally.

<https://doi.org/10.1016/j.redox.2023.102620>

Received 21 December 2022; Received in revised form 25 January 2023; Accepted 29 January 2023

Available online 1 February 2023

2213-2317/© 2023 The Authors. Published by Elsevier B.V. This is an open access article under the CC BY-NC-ND license (<http://creativecommons.org/licenses/by-nc-nd/4.0/>).

development of paraplegia is delayed in these patients, there is a window of opportunity for potential preventive intervention. However, no pharmacologic treatment has thus far been shown to mitigate delayed paraplegia after thoracoabdominal aortic surgery.

Hydrogen sulfide (H₂S), a colorless gas with a characteristic rotten-egg odor, is an environmental hazard produced by various natural and industrial sources. H₂S is also considered to be a signaling molecule, which plays diverse physiological roles [7]. Many effects of H₂S have been attributed to sulfane sulfur species such as persulfides (RSSH) and polysulfides (RS_nH) [8]. The cytoprotective effects of sulfane sulfur species may be mediated by multiple mechanisms, including antioxidant [9,10] and anti-inflammatory effects [10,11], inhibition of lipid peroxidation and ferroptosis by scavenging free radicals [12], and post-translational modifications of proteins [13,14]. Sulfane sulfur species produce post-translational modifications in proteins because the sulfane sulfur (S⁰), a sulfur atom with six valence electrons but no charge, is readily donated to acceptor thiols in target proteins in a process known as persulfidation, which modulates function of target proteins [13,14]. In a previous study, we showed that breathing H₂S prevents delayed paraplegia in mice subjected to transient spinal cord ischemia (SCI). The neuroprotective effects of H₂S appeared to be associated with persulfidation of nuclear factor-kappa B (NF-κB) p65 [15].

The mechanism by which systemically administered H₂S donor compounds modulate the concentration of reactive sulfur species in target tissue is poorly defined, in part because of the short half-life of H₂S in blood [16]. This knowledge gap, concerning the *in vivo* pharmacokinetics of sulfides, has hindered the application of sulfide-based therapies to patient care. To permit the future use of polysulfides for the treatment of neurodegenerative diseases, it is essential to determine whether administration of polysulfides modulates local concentrations of sulfane sulfur species in the central nervous system (CNS).

Glutathione trisulfide (GSSSG) is an endogenous polysulfide (Fig. 1A), and is in dynamic equilibrium with various reactive sulfur species including glutathione (GSH), glutathione hydropersulfide (GSSH), glutathione hydropolysulfides, and other glutathione

polysulfides [9,17]. GSSSG may be an important endogenous reservoir of sulfane sulfur species. The observation that the levels of sulfane sulfur species vary in patients, depending on the types and severity of diseases, suggests that sulfane sulfur species may have protective roles in pathological conditions [18,19].

GSH, which is a natural tripeptide of glutamate, cysteine, and glycine, is ubiquitous and is the most prevalent thiol (RSH) in mammalian cells. GSH is a nucleophile and acts as a major intracellular antioxidant in mammalian cells [20]. GSH has been reported to have neuroprotective effects against ischemia-reperfusion injury [21]. Glutathione disulfide (GSSG) is the oxidized form of GSH, and is predominantly produced by GSH peroxidase-mediated catalysis or from the direct reactions of GSH with electrophilic compounds such as radical species [20]. Both GSH and GSSG can produce post-translational modification of proteins by “glutathionylation”, which protects protein cysteines from irreversible oxidation and regulates the structure and function of a diverse range of proteins [20,22–24].

Pantethine (PTN), a precursor for the synthesis of coenzyme A, transfers acetyl groups from pyruvate to oxaloacetate, initiating the tricarboxylic acid cycle [25]. Preclinical studies suggested beneficial effects of PTN in mouse models of neurodegenerative diseases [26,27]. Pantethine trisulfide (PTN-SSS), a novel polysulfide, consists of one molecule of sulfane sulfur and one molecule of PTN (Fig. 1B).

The current study was designed to investigate the neuroprotective effects and pharmacokinetics of intranasal administration of polysulfides in a well-established mouse model of spinal cord ischemia. In this mouse model, neurodegeneration predominantly occurs in the ventral horn of lumbar spinal cord 24–48 h after reperfusion [6,28,29]. We anticipate that intranasal administration of polysulfides will preferentially increase levels of polysulfides in the CNS [30–32]. Accordingly, we hypothesized that CNS-targeted, intranasal administration of polysulfides will prevent neurodegeneration in the lumbar spinal cord by increasing the local concentration of sulfane sulfur species and will rescue mice from delayed paraplegia. Here, we report that, when delivered after reperfusion, GSSSG and PTN-SSS prevented delayed paraplegia after SCI. The neuroprotective effect of GSSSG was associated

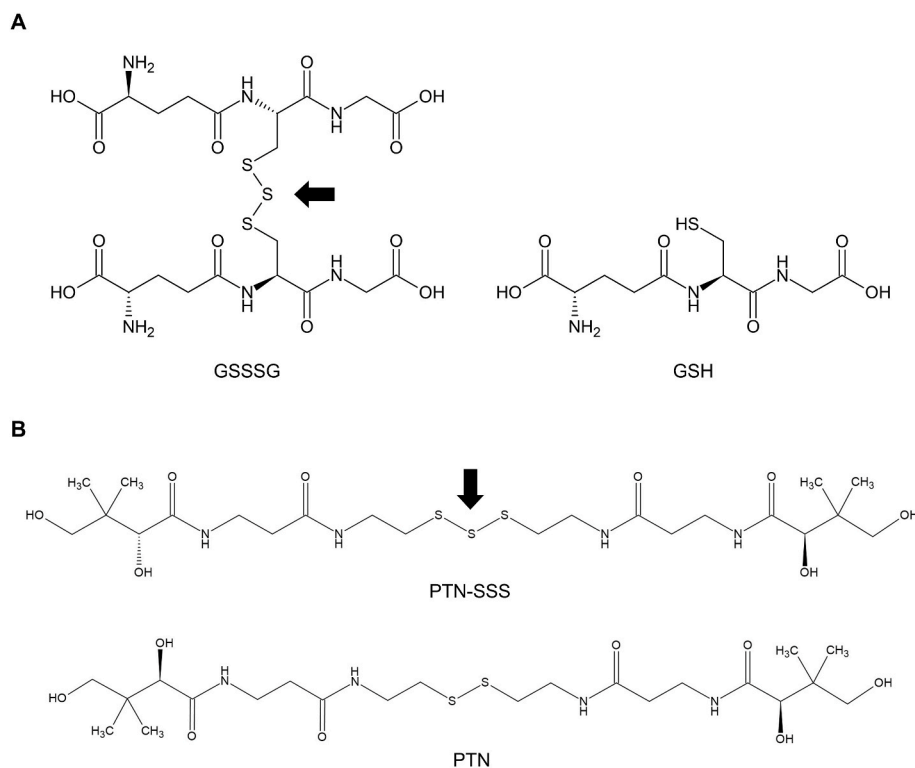


Fig. 1. Chemical structures of polysulfides A. Chemical structures of GSSSG and GSH. One molecule of GSSSG consists of one molecule of sulfane sulfur (arrow) and two molecules of GSH. B. Chemical structures of PTN-SSS and PTN. One molecule of PTN-SSS consists of one molecule of sulfane sulfur (arrow) and one molecule of PTN.

Abbreviations: GSH, glutathione; GSSSG, glutathione trisulfide; PTN, pantethine; PTN-SSS, pantethine trisulfide.

with increased local sulfane sulfur concentration in the lumbar spinal cord.

2. Materials and methods

2.1. Materials

A stable form of GSSSG dihydrate was synthesized and provided by Kyowa Hakko Bio Co., Ltd. (Tokyo, Japan). GSSSG was suspended in distilled water and dissolved by titrating the pH to between 4.8 and 5.0 with sodium bicarbonate (Sigma-Aldrich, Saint Louis, MO, USA). To avoid degradation of the compound, a fresh GSSSG solution was prepared immediately before each experiment. GSH (Sigma-Aldrich, Saint Louis, MO, USA) and GSSG hexahydrate (provided by Kyowa Hakko Bio Co., Ltd.) were dissolved in distilled water. In the GSSSG study, the vehicle alone was distilled water, with pH adjusted to between 4.8 and 5.0 with hydrochloric acid.

PTN-SSS was synthesized and provided by Kyowa Hakko Bio Co., Ltd. The purity of PTN-SSS is 96.3%, and PTN-SSS is highly water soluble (>50 g/L). PTN-SSS and PTN (Toronto Research Chemicals, Toronto, ON, Canada) were suspended in distilled water. PTN-SSS is stable in solution at pH 4.0–9.0 at room temperature for at least 4 days. In the PTN-SSS study, distilled water was used as the vehicle alone.

2.2. In vivo studies

2.2.1. Animals

All animal procedures were performed in accordance with protocols approved by Massachusetts General Hospital Institutional Animal Care and Use Committee and National Research Council's "Guide for the Care

and Use of Laboratory Animals". The study design and the description of experiments followed the ARRIVE guidelines. Adult C57BL/6J mice (12–18 weeks old) of both sexes were purchased from Jackson Laboratory (Bar Harbor, ME, USA). Both male and female mice were used in experiments to investigate the neuroprotective effect of GSSSG on motor function after SCI. Because the neuroprotective effects of GSSSG appeared to be independent of sex, subsequent *in vivo* experiments were performed in male mice only. All mice were housed in a temperature and humidity-controlled room in the animal center with a 12-h light/dark cycle, and were provided with food and water *ab libitum*. To permit access by mice that were recovering from surgery, additional food pellets were inserted into hydrated gel placed on the bedding. A randomized paired design was used to minimize the variability between each treatment group. Mice were paired based on weight, age, delivery dates, and when possible, holding cages. After the pairing, mice were randomly assigned to different treatments.

2.2.2. Surgery to induce spinal cord ischemia and administration of study drugs

The surgical procedures to produce delayed paraplegia in mice were performed as previously described [6] (Fig. 2A). Mice were anesthetized with 5% isoflurane in 100% O₂ and tracheally intubated with a 20-gauge catheter (Angiocath; Becton Dickinson, Franklin Lakes, NJ, USA). Mice were mechanically ventilated (MiniVent model 845; Harvard Apparatus, Holliston, MA, USA) and anesthesia was maintained with 2% isoflurane in 100% O₂, with tidal volume 8 μ l/g. The paravertebral muscle temperature was measured using a T-type implantable thermocouple probe (IT-18) and a T-type pod (ADInstruments, Colorado Springs, CO, USA). After a skin incision was made on the back, the tip of the probe was placed at the level of L1-L3 using an 18-gauge needle and the

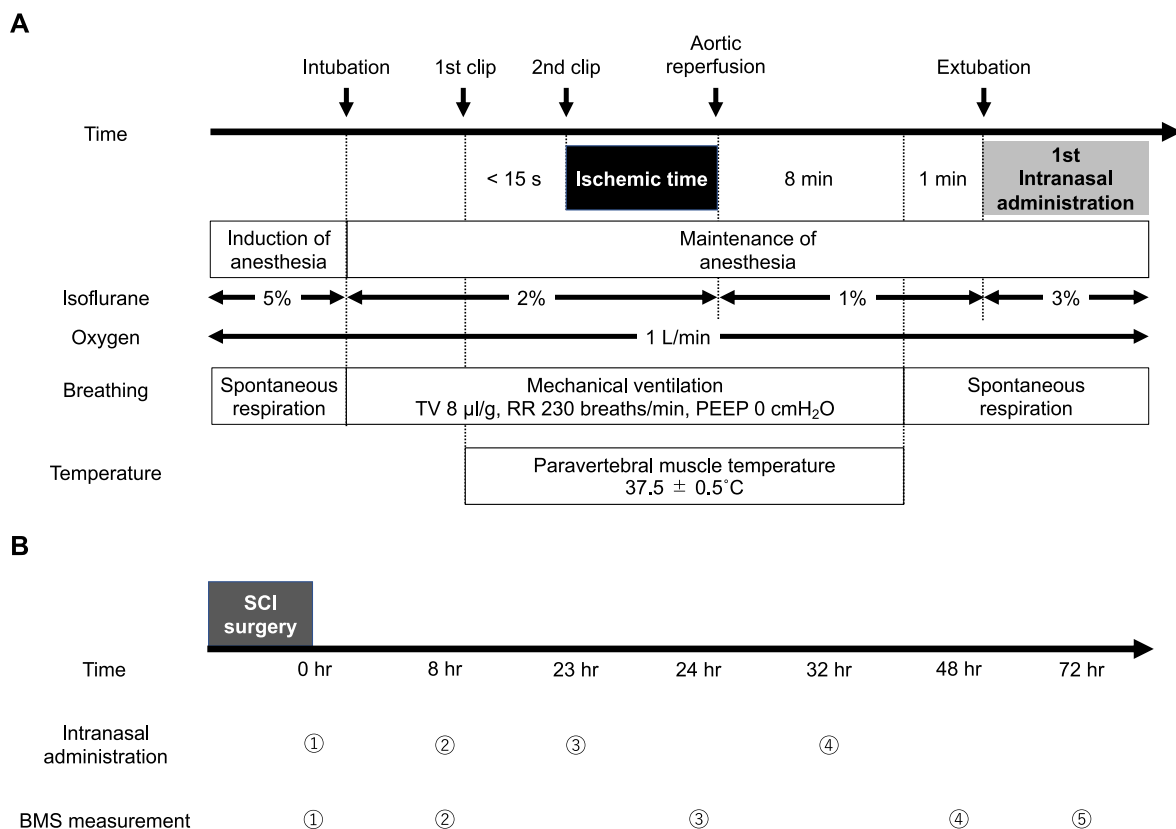


Fig. 2. A mouse model of spinal cord ischemia-reperfusion injury to investigate the neuroprotective effects of polysulfide. **A.** A schematic diagram of time course of surgical procedure to produce delayed paraplegia. SCI was induced by clamping the distal aortic arch and the left subclavian artery. **B.** The protocol for intranasal administration of study drugs after the surgical procedure and restoration of perfusion. The intranasal administration of study drugs was conducted under 3% isoflurane at 0, 8, 23, and 32 h after surgery. BMS was measured at 0, 8, 24, 48, and 72 h after surgery to evaluate the hindlimb motor function. Abbreviations: BMS, Basso mouse scale for locomotion; PEEP, positive end-expiratory pressure; RR, respiratory rate; SCI, spinal cord ischemia; TV, tidal volume.

temperature was maintained at 37.5 ± 0.5 °C using a heating pad and DC temperature controller (FHC, Bowdoin, ME, USA). A median sternotomy extended from the apex of the manubrium to the second rib. The aortic arch was gently isolated between the left common carotid artery (LCCA) and the left subclavian artery (LSA), avoiding the vagus nerve and the left recurrent laryngeal nerve. A first clip (straight micro clip, RS-5424; Roboz Surgical Instrument Company, Inc., Gaithersburg, MD, USA) was placed on the aortic arch between the LCCA and LSA, and then, within 15 s, a second clip (45° angle micro clip, RS-5435; Roboz Surgical Instrument Company, Inc., Gaithersburg, MD, USA) was placed on the origin of the LSA. After ischemia, the clips were removed in reverse order. Incisions were closed in layers and mechanical ventilation was discontinued. After stable spontaneous respiration was confirmed, mice were extubated.

The previously described surgical procedures [6] were modified as follows. The respiratory rate during the procedure was increased to 230 breaths/minute, because hyperventilation promotes the occurrence of delayed paraplegia caused by spinal cord ischemia [33]. A laser Doppler perfusion monitor (moorVMS-LDF1; Moor Instruments, Millwey, UK) was used to monitor the femoral artery blood flow [28,29]. A plastic fiber (POF500; Moor Instruments, Millwey, UK) was affixed perpendicular to the left femoral artery, to confirm that occlusion of aorta resulted in an immediate and sustained reduction (>90%) in the femoral artery blood flow [28,29]. To improve the accuracy of surgical procedures, a microscope (Leica MZ95; Leica Microsystems, Buffalo Grove, IL, USA) was used to isolate the aortic arch and place the clips. Based on the results of pilot studies, we selected the ischemic time which induced delayed paraplegia in all mice (3 min for male mice, 3.5 min for female mice) with the lowest mortality rate at 72 h after surgery (Table S1).

Study drugs were administered intranasally using a single-channel pipettor. Mice were anesthetized with 3% isoflurane using a non-rebreathing circuit with a mouse nose cone (VetEquip, Inc., Livermore, CA, USA). While the drugs were administered, the nose cone was removed and mice were allowed to breathe air. Approximately 6 μ L of each drug was administered into the mouse's nostrils and the mouse inhaled the droplets during inspiration. This procedure was repeated at intervals until the total volume of drug was administered, which took approximately 10 min. The interruption time of isoflurane administration for each intranasal dose was about 10 s. The intranasal drugs were administered 0, 8, 23, and 32 h after surgery (Fig. 2B). In the sham procedure group, the surgical procedures described above were conducted, but the aorta was not cross-clamped.

For pain control, 0.1 mg/kg of buprenorphine was administered intraperitoneally before surgery and every 12 h until 60 h after surgery. We also administered 0.5 mg/kg of 0.25% bupivacaine subcutaneously around the wound incision site immediately after surgery.

2.2.3. Assessment of motor function after spinal cord ischemia

The hindlimb motor function was quantified using the Basso mouse scale for locomotion (BMS) [34] at 0, 8, 24, 48, and 72 h after surgery (Fig. 2B). This score ranges from 0 for complete paraplegia to 9 for normal motor function. A BMS score < 6 (0–5) indicates paraplegia or paraparesis, whereas a BMS score \geq 6 (6–9) indicates that mice are able to walk.

2.2.4. Studies to investigate the neuroprotective effect of post-perfusion treatment with GSSSG on motor function after spinal cord ischemia

Mice were randomly assigned to each treatment group and the investigator who performed the surgical procedure was blinded to the group assignment. Based on pilot studies, 50 mg/kg of GSSSG, 45.2 mg/kg of GSH (twice the molar amount of GSSSG because one molecule of GSSSG contains two molecules of GSH) (Fig. 1A), or 53 mg/kg of GSSG (an equimolar dose of GSSSG) was administered.

2.2.5. Histological studies

The lumbar enlargement of the spinal cord was removed 48 h after

surgery and sectioned to 5 μ m thickness using a cryotome (CM1850UV; Leica Biosystems, Heidelberg, Germany). Nissl staining was conducted using the Nissl stain kit (VivoVivo Biotech, Rockville, MD, USA) according to the protocol recommended by the manufacturer. Immunohistochemical staining for ionized calcium-binding adaptor molecule 1 (Iba-1) and cleaved caspase-3 was performed as previously described [6, 15]. The stained sections were examined using an epifluorescence microscope (Nikon Eclipse 80i; Nikon Instruments, Inc., Melville, NY, USA).

The number of stained cells was counted in one field (0.26 mm²) under high magnification (200 \times) in 3 different sections of spinal cord from each mouse by an investigator who was blinded to the identity of the samples. The average number of stained cells was calculated for each mouse. For quantitative analysis of Iba-1 staining, the Iba-1-positive area per one field (0.26 mm²) under high magnification (200 \times) in 3 different ventral horn sections for each mouse was calculated using the ImageJ image-processing program (National Institutes of Health, Bethesda, MD, USA). The mean area of Iba-1 staining in the spinal cords of mice in the sham procedure group was set to 1 and the relative amount of Iba-1 staining was determined for each experimental group of mice. Each group included 5 mice.

2.2.6. Measurements of gene expression

Messenger RNA (mRNA) levels were measured as previously described [15] using lumbar spinal cords at 48 h after surgery. The mRNA levels of C-C motif chemokine 2 (CCL2), C-X-C motif chemokine ligand 1 (CXCL1), interleukin (IL)-1 β , IL-6, tumor necrosis factor (TNF)- α , B-cell lymphoma 2 (Bcl-2), B-cell lymphoma-extra large (Bcl-XL), cystathionine beta synthase, cystathionine gamma lyase, 3-mercaptopyruvate sulfurtransferase, sulfide:quinone oxidoreductase (SQOR), ethylmaronic encephalopathy 1, thiosulfate sulfurtransferase, sulfite oxidase, cysteinyl-tRNA synthetase 1, and cysteinyl-tRNA synthetase 2 were standardized to the level of 18S ribosomal RNA using quantitative real-time polymerase chain reaction (7500 Fast Real-Time PCR System, Thermo Fisher Scientific, Waltham, MA, USA). Primer sequences are listed in Table S2.

2.2.7. Liquid chromatography-tandem mass spectrometry (LC-MS/MS) analysis

We used LC-MS/MS analysis to measure the amount of ³⁴S-labeled GSSSG ([³²S₂, ³⁴S]GSSSG) in the CNS and plasma after intranasal administration of GS³⁴SSG, an isotope of endogenous GSSSG [9,35,36]. The ratios of ³⁴S-labeled sulfane sulfur species ([³²S, ³⁴S]GSSH, [³²S, ³⁴S]cysteine hydropersulfide (CysSSH), and [³²S₂, ³⁴S]cysteine trisulfide (CysSSSCys)) to endogenous sulfane sulfur species ([³²S₂]GSSH, [³²S₂]CysSSH, and [³²S₃]CysSSSCys) were also quantitatively evaluated. At 30 min after intranasal administration of 50 mg/kg of GS³⁴SSG, blood was obtained and four different central nervous tissues were harvested: olfactory bulb and forebrain; brainstem; cervical and thoracic spinal cord, and lumbar spinal cord. A total of 30 mg of each tissue was homogenized in 300 μ L of ice-cold methanol solution containing 5 mM β -(4-hydroxyphenyl)ethyl iodoacetamide (HPE-IAM; Santa Cruz Biotechnology, Dallas, TX, USA). Twenty-five μ L of plasma was mixed with 75 μ L of ice-cold methanol solution containing 5 mM HPE-IAM. Samples were incubated for 20 min at 37 °C in the dark. After centrifugation (14,000 \times g for tissues, 1,870 \times g for plasma, 10 min, 4 °C), the supernatant was separated and diluted with 0.1% formic acid for LC-MS/MS analysis, and the pellet was sonicated to measure the protein concentration by BCA assay. The amount of [³²S₂, ³⁴S]GSSSG was quantified in selective reaction monitoring (SRM) with precursor ion (647.14 *m/z*), product ion (389.1 *m/z*), and higher energy collisional dissociation (21 *v*). The ratios of [³²S, ³⁴S]GSSH to [³²S₂]GSSH, [³²S, ³⁴S]CysSSH to [³²S₂]CysSSH, and [³²S₂, ³⁴S]CysSSSCys to [³²S₃]CysSSSCys were calculated from their peak area measured by Dionex UltiMate 3000 RS UPLC-Orbitrap Exploris 480 mass spectrometer (Thermo Fisher Scientific, Waltham, MA, USA). In brief, samples were

subjected to the UPLC system with a Hypersil Gold C-18 (100 × 2.1 mm, 3.0 μm, Thermo Fisher Scientific, Waltham, MA, USA) column and were then eluted by a linear methanol gradient of the mobile phase (0–90%, 15 min) in the presence of 0.1% formic acid at a flow rate of 0.2 ml/min at 40 °C. The raw data were analyzed by Compound Discoverer 3.3 software (Thermo Fisher Scientific, Waltham, MA, USA). The molecular weights of these sulfane sulfur species combined with HPE-IAM were determined based on previous reports [9,11,37].

2.2.8. Measurements of relative sulfane sulfur levels in lumbar spinal cords after spinal cord ischemia

Lumbar spinal cords were harvested 48 h after surgery and snap-frozen in liquid nitrogen. Spinal cords were subsequently homogenized in Hanks' balanced salt solution (HBSS; Thermo Fisher Scientific, Waltham, MA, USA) containing SSip-1 (5 μM), incubated at room temperature in the dark for 20 min, and then subjected to centrifugation. SSip-1 was synthesized and provided by the Hanaoka laboratory [38]. The fluorescence intensities of supernatants were measured using a microplate reader (SpectraMax M5; Molecular Devices, San Jose, CA, USA) at the wavelength of $\lambda_{ex}/\lambda_{em}$ = 491 nm/525 nm. The fluorescence intensities were normalized to the weights of the spinal cord.

2.2.9. Measurements of relative sulfane sulfur levels in olfactory bulb and forebrain, and whole spinal cord after intranasal administration of PTN-SSS

At 30 min after intranasal administration of 50 mg/kg of PTN-SSS, the olfactory bulb and forebrain and the whole spinal cord were harvested. Tissues were homogenized in HBSS containing 10 μM of SSip-1. The fluorescence intensities of supernatants were measured.

2.3. In vitro studies

2.3.1. Murine primary cortical neuron culture

Primary cortical neurons were isolated from the cerebral cortices of C57BL/6J mice of both sexes at embryonic day 15, as previously described [39]. Primary cortical neurons were maintained at 37 °C in a humidified tissue culture chamber with 5% CO₂ and cells were used on day 11 after harvest.

2.3.2. Measurements of relative sulfane sulfur levels in primary cortical neurons or SH-SY5Y cells after incubation with polysulfides

Primary cortical neurons or SH-SY5Y cells, a human neuroblastoma cell line (American Type Culture Collection, Manassas, VA, USA), were incubated with SSip-1 DA (5 μM) [38] at 37 °C for 20 min in the dark. Cells were washed with pre-warmed HBSS containing calcium and magnesium (Thermo Fisher Scientific, Waltham, MA, USA) and then cells were incubated with GSSSG, sodium trisulfide (Na₂S₃; Dojindo Molecular Technologies, Inc., Rockville, MD, USA), PTN-SSS, or vehicle alone for 20 min at 37 °C in the dark. Fluorescence intensities were measured using a microplate reader.

2.3.3. Effect of polysulfides on cell viability after oxygen and glucose deprivation/reoxygenation (OGD/R)

After primary cortical neurons or SH-SY5Y cells were subjected to 2.5 or 15 h of OGD in an incubation chamber (MIC-101; Billups-Rothenberg, Inc., San Diego, CA, USA), the cells were incubated with GSSSG, GSH, GSSG, PTN-SSS, or vehicle only, and then subjected to 21- (primary cortical neurons) or 24- (SH-SY5Y cells) h of reoxygenation, as previously described [39]. After reoxygenation, cell viability and cell injury were assessed using crystal violet and lactate dehydrogenase (LDH) assays, as previously described [39].

2.3.4. Cytotoxic effect of GSSSG on cell viability

Primary cortical neurons were incubated for 21 h with GSSSG at 0 μM (vehicle alone), 10 μM, 30 μM, 60 μM, or 100 μM in a humidified incubator with 95% air and 5% CO₂ at 37 °C. Cell viability was assessed using the LDH assay.

2.3.5. Cytotoxic effect of PTN-SSS on cell viability

SH-SY5Y cells were incubated for 24 h with PTN-SSS at 0 μM (vehicle alone), 5 μM, 10 μM, 25 μM, 50 μM, or 100 μM in a humidified incubator with 95% air and 5% CO₂ at 37 °C. Cell viability was assessed using the crystal violet assay.

2.4. Statistical analysis

Data are presented as means with standard deviation (parametric data) or medians with interquartile range (nonparametric data). Descriptive statistics were used to describe the study population. We used Shapiro-Wilk test and Q-Q plots to assess the normality of the data. Parametric data were analyzed using unpaired *t*-test to compare two groups, and one-way analysis of variance (ANOVA) with Tukey's multiple comparison test or Dunnett's multiple comparison test to compare three or more groups. Non-parametric data were analyzed using Mann-Whitney test to compare two groups, and Kruskal-Wallis test with Dunn's multiple comparisons test to compare three or more groups. The significance was considered at the level of *P* < 0.05. Statistical analyses were conducted using GraphPad Prism 9.2.0 (GraphPad Software Inc., San Diego, CA, USA).

The sample size calculation of the experiment to compare the BMS scores at 72 h after surgery between GSSSG, GSH, and vehicle alone groups was conducted using F test for the fixed effects one-way ANOVA (G*Power 3.1; Heinrich-Heine-Universität, Düsseldorf, Germany) [40]. We presumed that 11 mice for male mice and 8 mice for female mice per group would be required based on our pilot studies for this experiment ($\alpha = 0.05$, $\beta = 0.1$ [Power = 0.9], effect size $f = 0.7022756$ for male mice and $f = 0.8709832$ for female mice, number of groups = 3). The sample size calculation of the experiment to compare the BMS scores at 72 h after surgery between PTN-SSS, PTN, and vehicle alone groups was conducted using F test for the fixed effects one-way ANOVA. We presumed that 9 mice per group would be required based on our pilot studies for this experiment ($\alpha = 0.05$, $\beta = 0.1$ [Power = 0.9], effect size $f = 0.7747206$, number of groups = 3).

3. Results

3.1. Intranasal administration of GSSSG rescued mice from delayed paraplegia after transient spinal cord ischemia

To investigate whether polysulfides can prevent delayed paraplegia, mice were subjected to SCI and were treated with GSSSG, GSH, or vehicle alone 0, 8, 23, and 32 h after surgery. Thirty-six male mice were subjected to SCI; however, three of these mice were excluded from further study because a greater than 90% reduction in the femoral artery blood flow was not achieved. The remaining 33 male mice received one of three treatments: GSSSG (*n* = 11), GSH (*n* = 11), or vehicle alone (*n* = 11). The hindlimb motor function was quantified using the Basso mouse scale for locomotion (BMS), which evaluates hindlimb movement, forelimb-hindlimb coordination, and trunk stability. As previously described by Kakinohana and colleagues, if the neurologic deficit (BMS < 6) occurred after a period during which a mouse was able to walk (BMS ≥ 6), then the mouse was considered to have delayed paraplegia [6].

Beginning approximately 36 h after surgery, the hindlimb motor function of mice treated with vehicle alone gradually worsened and all of the mice treated with vehicle alone developed paraplegia by 48 h after surgery (Fig. 3). In contrast, intranasal administration of GSSSG prevented the development of delayed paraplegia in 8 of 11 mice (73%) and, compared to vehicle alone, improved the BMS score at 72 h after surgery (GSSSG vs vehicle alone, BMS; 9 [4–9] vs 0 [0–0]; *P* < 0.0001 by Kruskal-Wallis test with Dunn's multiple comparisons test, Fig. 3). Intranasal administration of GSH also prevented delayed paraplegia in 3 of 11 mice (27%), but did not improve the BMS score at 72 h after surgery (GSH vs vehicle alone, BMS; 1 [0–7] vs 0 [0–0]; *P* = 0.0914,

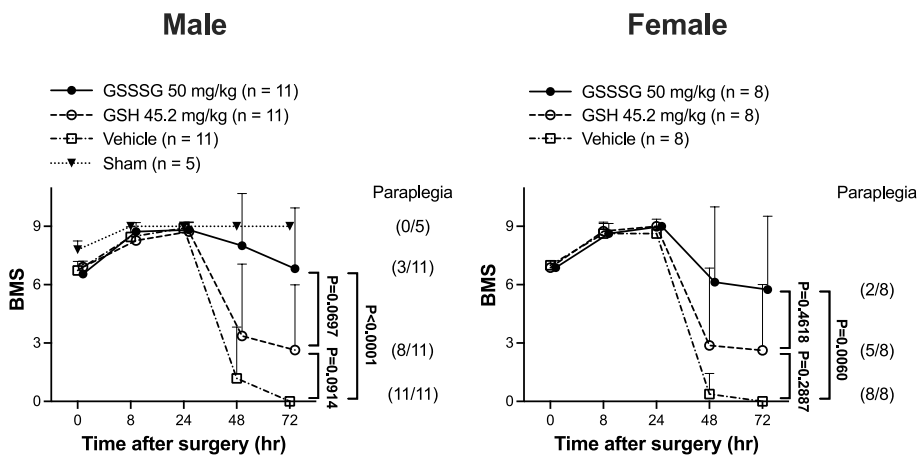


Fig. 3. The results show that GSSSG, but not GSH, prevents the development of delayed paraplegia after SCI in male mice.

To investigate the effect of sex on the ability of GSSSG to prevent delayed paraplegia after SCI, 28 female mice were subjected to SCI and were treated with GSSSG, GSH, or vehicle alone 0, 8, 23, and 32 h after surgery. Four of the 28 female mice experienced labored breathing immediately after extubation and were euthanized. The remaining 24 female mice were treated with GSSSG ($n = 8$), GSH ($n = 8$), or vehicle alone ($n = 8$). Compared to mice treated with vehicle alone, mice that received intranasal GSSSG had an improved BMS scores at 72 h after surgery (GSSSG vs vehicle alone, BMS; 6.5 [1.5–9.0] vs 0.0 [0.0–0.0]; $P = 0.0060$ by Kruskal-Wallis test with Dunn's multiple comparisons test, Fig. 3). In contrast, intranasal administration of GSH did not improve the BMS scores at 72 h after surgery (GSH vs vehicle alone, BMS; 0.5 [0.0–6.7] vs 0.0 [0.0–0.0]; $P = 0.2887$, Fig. 3). These results show that GSSSG, but not GSH, is able to prevent delayed paraplegia after SCI in both sexes.

GSSG can react with thiols in proteins by glutathionylation ($\text{PSH} + \text{GSSG} \rightleftharpoons \text{PSSG} + \text{GSH}$) [23]. GSSSG potentially can also react with thiols in proteins by the same process [41]. To investigate whether the beneficial effects of GSSSG are related to glutathionylation, we compared the effects of intranasal administration of GSSSG or GSSG on outcomes after SCI in male mice. Intranasal administration of GSSSG rescued 5 out of 6 male mice (83%) from delayed paraplegia; in contrast, intranasal administration of GSSG did not rescue any male mouse from delayed paraplegia (0%). The BMS score at 72 h after surgery in the GSSSG group was significantly higher than that in the GSSG group (GSSSG vs GSSG, BMS; 8.0 [5.2–9.0] vs 0.0 [0.0–0.0]; $P = 0.0152$ by Mann Whitney test, Fig. S1). Because GSSSG potentially can mediate glutathionylation of target proteins by the same process as GSSG, but only GSSSG protects against delayed paraplegia, the results suggest that the neuroprotective effects of GSSSG are not a result of glutathionylation.

3.2. Intranasal administration of GSSSG decreased neurodegeneration and microglial- and caspase-3- activation after spinal cord ischemia in lumbar spinal cords

Spinal cord ischemia is associated with degenerative changes in neurons in the ventral horn of the lumbar spinal cord and the viability of affected neurons can be assessed using Nissl staining [6]. Nissl stain detects Nissl bodies in the cytoplasm of neurons and the presence of this purple, cytoplasmic staining is an indicator of neuronal integrity [6,42]. To investigate the effects of GSSSG on neurodegeneration, GSSSG or vehicle alone was administered 0, 8, 23, and 32 h after surgery. Lumbar spinal cords were harvested 48 h after surgery, fixed, sectioned, and incubated with Nissl stain. Compared to mice undergoing a sham surgical procedure, spinal cord ischemia was associated with a marked

Fig. 3. Post-reperfusion treatment with GSSSG prevented paraplegia after spinal cord ischemia in male and female mice. Changes in BMS scores for 72 h after SCI in male and female mice subjected to a sham surgical procedure, or SCI and treated with GSSSG, GSH, or vehicle alone. $n = 11$ for each of the GSSSG, GSH, and vehicle alone treatments in the male mouse cohort, and $n = 8$ for each of the GSSSG, GSH, and vehicle alone treatments in the female mouse cohort. $n = 5$ mice for the sham surgical group. Data are presented as means with standard deviation. Abbreviations: BMS, Basso mouse scale for locomotion; GSH, glutathione; GSSSG, glutathione trisulfide; SCI, spinal cord ischemia.

decrease in neurons that were positive for Nissl stain, suggesting that the majority of cells were not viable (Fig. 4). Compared to mice that underwent SCI and were treated with vehicle alone, intranasal administration of GSSSG was associated with a significant increase in the number of viable neurons (Fig. 4).

Previous studies showed that increased microglial activation in the ventral horn of the lumbar spinal cord parallels the onset of delayed paraplegia after SCI [6,29], and inhibition of microglial activation attenuates neuronal injury and prevents the development of delayed paraplegia after SCI [43]. Increased expression of Ionized calcium-binding adapter molecule 1 (Iba-1) is a sensitive marker for activation of microglia [44]. To explore the mechanisms by which GSSSG prevents neurodegeneration, mice were subjected to SCI and treated with GSSSG or vehicle alone. Sections were prepared from the lumbar spinal cord and were stained for Iba-1. Compared to the staining of the spinal cord obtained from mice 48 h after a sham operation, the staining of the spinal cord from mice that were subjected to SCI had a markedly increased relative area of Iba-1-positive staining (Fig. 5A and B). The results indicate that SCI is associated with increased activation of microglia. In contrast, mice that underwent SCI and were treated with intranasal GSSSG had a significant reduction in staining for Iba-1, indicating decreased microglial activation (Fig. 5A and B).

Previous investigators showed that activation of caspase-3 is a central component of the neurodegeneration that occurs in the ventral horn of the lumbar spinal cord after SCI [6]. Immunohistochemical staining for cleaved caspase-3 was used to investigate whether attenuation of caspase-3 activation may be a mechanism by which GSSSG prevents neurodegeneration after SCI. Compared to spinal cords from mice 48 h after a sham operation, the lumbar spinal cords from mice that were subjected to SCI had an increased number of cleaved caspase-3-positive neurons in the ventral horns (Fig. 5C and D). Intranasal administration of GSSSG prevented the SCI-induced increase in the number of cleaved caspase-3-positive neurons in lumbar spinal cord (Fig. 5C and D). These results suggest that the intranasal administration of GSSSG prevents neurodegeneration in the ventral horn of the lumbar spinal cord and is associated with decreased microglial activation and attenuation of caspase-3 activation.

3.3. Intranasal administration of GSSSG attenuated upregulation of pro-inflammatory cytokines after spinal cord ischemia

Previous studies showed that a marked increase in pro-inflammatory cytokines produced by activated microglia precedes the onset of delayed paraplegia after SCI [15,29]. Inhibition of microglial activation suppresses the upregulation of pro-inflammatory cytokines and prevents the development of delayed paraplegia after SCI [43]. To further assess the effect of GSSSG on pro-inflammatory cytokines induced by SCI, we

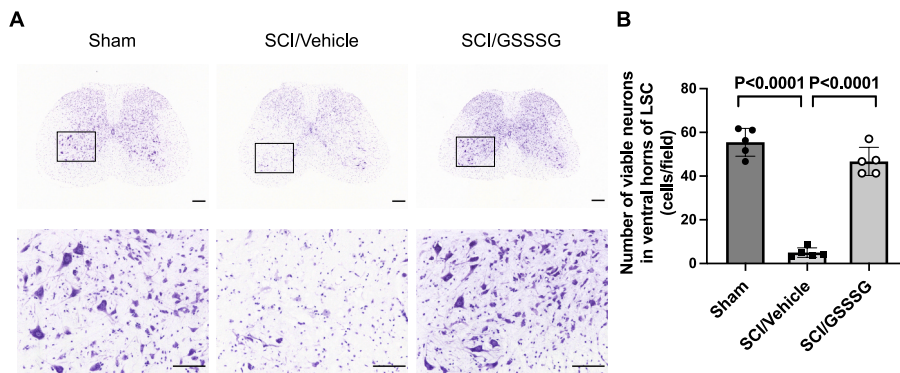


Fig. 4. Post-reperfusion treatment with GSSSG prevented loss of motoneurons in lumbar spinal cord at 48 h after spinal cord ischemia. **A.** Representative photomicrographs of Nissl-stained lumbar spinal cord cross-sections from mice subjected to a sham surgical procedure, or SCI and treated with GSSSG or vehicle alone. An enlargement of the boxed regions is provided below each cross-section. Scale bar = 200 μ m in low magnification images (40 \times) and 100 μ m in high magnification images (200 \times). **B.** Number of viable neurons per one field (0.26 mm²) under high magnification (200 \times) in the ventral horns of lumbar spinal cord sections from mice subjected to a sham surgical procedure, or SCI and treated with vehicle alone, or GSSSG. Comparisons were made using one-way ANOVA with Tukey's multiple comparison test. n = 5 mice for each group. Data are

presented as means with standard deviation.

Abbreviations: GSSSG, glutathione trisulfide; LSC, lumbar spinal cord; SCI, spinal cord ischemia.

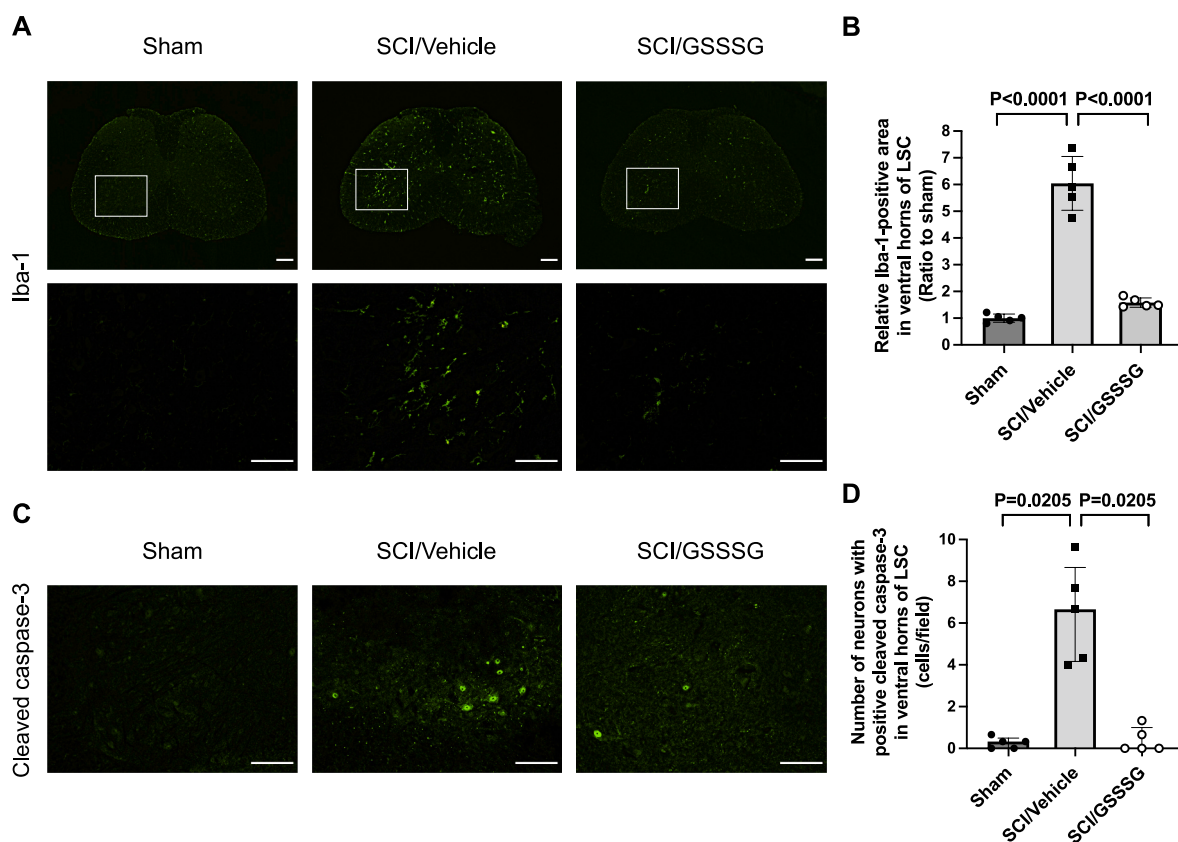


Fig. 5. Post-reperfusion treatment with GSSSG prevented microglial activation and caspase-3 activation in lumbar spinal cord at 48 h after spinal cord ischemia. **A.** Lumbar spinal cords were obtained from mice subjected to a sham surgical procedure, or SCI and treated with GSSSG or vehicle alone. Representative photomicrographs of lumbar spinal cord cross-sections stained with anti-Iba-1 antiserum are shown. An enlargement of the boxed regions is provided below each cross-section. Scale bar = 200 μ m in low magnification images (40 \times) and 100 μ m in high magnification images (200 \times). **B.** Iba-1-positive area per one field (0.26 mm²) under high magnification (200 \times) in the ventral horns of lumbar spinal cord sections from mice subjected to a sham surgical procedure, or SCI and treated with GSSSG or vehicle alone. Comparisons were made using one-way ANOVA with Tukey's multiple comparison test. The mean value of the Iba-1-positive area in mice in the sham group was set to 1. n = 5 mice for each group. Data are presented as means with standard deviation. **C.** Representative photomicrographs of the ventral horn in lumbar spinal cord cross-sections stained with antibodies that recognize cleaved caspase-3. Scale bar = 100 μ m. **D.** Number of neurons with positive cleaved caspase-3 immunoreactivity per one field (0.26 mm²) under high magnification (200 \times) in the ventral horn of lumbar spinal cord sections. Comparisons were made using Kruskal-Wallis test with Dunn's multiple comparisons test. n = 5 mice for each group. Data are presented as medians with an interquartile range. Abbreviations: GSSSG, glutathione trisulfide; Iba-1, ionized calcium binding adaptor molecule 1; LSC, lumbar spinal cord; SCI, spinal cord ischemia.

measured the levels of mRNA encoding CCL2, CXCL1, IL-1 β , IL-6, and TNF- α in lumbar spinal cords from mice that were subjected to SCI and treated with GSSSG or vehicle alone. Lumbar spinal cords were harvested 48 h after surgery. Compared to mice that underwent a sham operation, mice that were subjected to SCI had a marked increase in the

levels of mRNAs encoding cytokines associated with inflammation. In contrast, GSSSG attenuated the upregulation of mRNA encoding pro-inflammatory cytokines 48 h after surgery (Fig. 6). The intranasal administration of GSSSG also decreased the level of mRNA encoding SQOR, an enzyme that oxidizes sulfides to persulfides. GSSSG had no

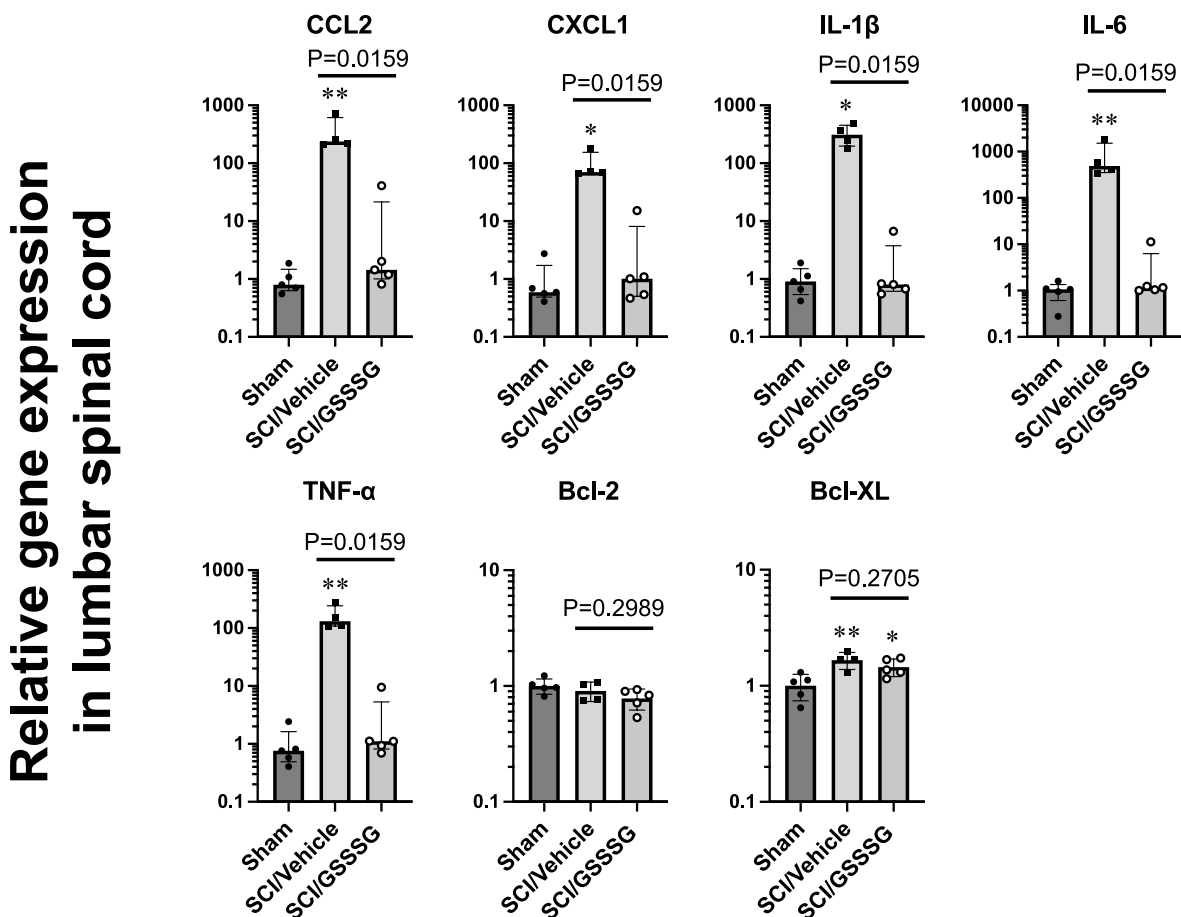


Fig. 6. Post-reperfusion treatment with GSSG inhibited upregulation of inflammatory mediators in lumbar spinal cord at 48 h after spinal cord ischemia. Mice underwent a sham surgical procedure or SCI followed by intranasal administration of GSSG or vehicle alone. Lumbar spinal cords were harvested and the mRNA levels for each gene were normalized to 18S ribosomal RNA. The mean value of lumbar spinal cord mRNA levels in mice in the sham group was set to 1. $n = 4-5$ mice for each group. * $P < 0.05$, ** $P < 0.01$ vs Sham. Data are presented as medians with interquartile range for CCL2, CXCL1, IL-1 β , IL-6, and TNF- α , and as means with standard deviation for Bcl-2 and Bcl-XL.

Abbreviations: Bcl-2, B-cell lymphoma 2; Bcl-XL, B-cell lymphoma-extra large; CCL2, C-C motif chemokine 2; CXCL1, C-X-C motif chemokine ligand 1; GSSG, glutathione trisulfide; IL, interleukin; mRNA, messenger RNA; SCI, spinal cord ischemia; TNF- α , tumor necrosis factor- α .

effect on mRNA levels encoding other enzymes that synthesize or metabolize sulfides or persulfides (Fig. S2). There was no significant difference between vehicle alone and GSSG treatment groups in mRNA

levels of anti-apoptotic genes including Bcl-2 and Bcl-XL (Fig. 6). These results suggest that the beneficial effects of GSSG may be mediated by inhibition of pro-inflammatory cytokines.

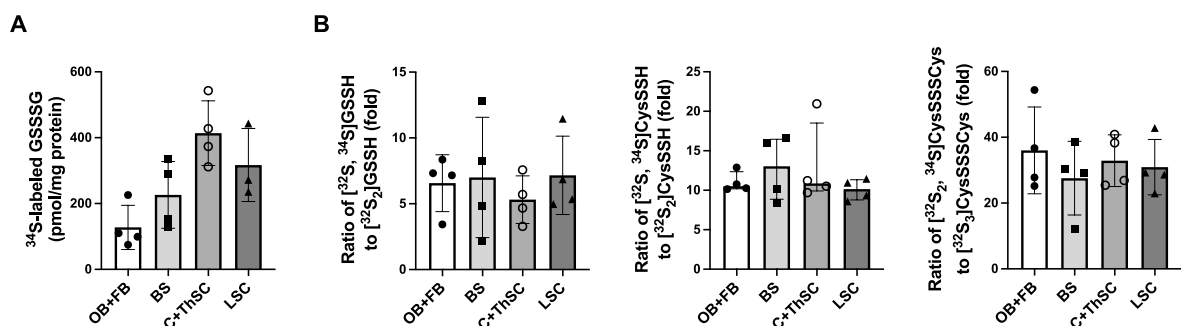


Fig. 7. Intranasal administration of GS 34 SSG increased levels of ^{34}S -labeled GSSG and ratios of ^{34}S -labeled sulfane sulfur species to endogenous sulfane sulfur species in CNS. A. Amount of ^{34}S -labeled GSSG detected in OB + FB, BS, C + ThSC, and LSC at 30 min after intranasal administration of 50 mg/kg of GS 34 SSG. $n = 4$ mice for OB + FB, BS, and C + ThSC. $n = 3$ mice for LSC. Data are presented as means with standard deviation. B. Ratios of [^{32}S , ^{34}S]GSSH to [$^{32}\text{S}_2$]GSSH, [^{32}S , ^{34}S]CysSSH to [$^{32}\text{S}_2$]CysSSH, and [^{32}S , ^{34}S]CysSSSCys to [$^{32}\text{S}_3$]CysSSSCys in OB + FB, BS, C + ThSC, and LSC at 30 min after intranasal administration of 50 mg/kg of GS 34 SSG. $n = 4$ mice for each organ. Data are presented as means with standard deviation for the ratios of [^{32}S , ^{34}S]GSSH to [$^{32}\text{S}_2$]GSSH and [^{32}S , ^{34}S]CysSSSCys to [$^{32}\text{S}_3$]CysSSSCys, and as medians with interquartile range for the ratio of [^{32}S , ^{34}S]CysSSH to [$^{32}\text{S}_2$]CysSSH.

Abbreviations: BS, brainstem; CNS, central nervous system; C + ThSC, cervical and thoracic spinal cord; CysSSH, cysteine hydropersulfide; CysSSSCys, cysteine trisulfide; GSSH, glutathione hydropersulfide; GSSG, glutathione trisulfide; LC-MS/MS, Liquid chromatography-tandem mass spectrometry; LSC, lumbar spinal cord; OB + FB, olfactory bulb and forebrain.

3.4. ^{34}S -labeled GSSSG reached the spinal cord shortly after intranasal administration and was metabolized to other sulfane sulfur species

To study the pharmacokinetics of intranasally-administered GSSSG, we used ^{34}S -labeled GSSSG to investigate the distribution of GSSSG and its metabolites (GSSH, CysSSH, and CysSSSCys) in the CNS after intranasal administration. Thirty minutes after intranasal administration of $^{32}\text{S}_2$, ^{34}S GSSSG, and to determine the ratios of ^{34}S -labeled sulfane sulfur species to endogenous sulfane sulfur species, in brain, spinal cord, and plasma. [$^{32}\text{S}_2$, ^{34}S]GSSSG was detected in olfactory bulb and forebrain (128 ± 67 pmol/mg protein), brainstem (226 ± 101 pmol/mg protein), cervical and thoracic spinal cord (414 ± 98 pmol/mg protein), and lumbar spinal cord (317 ± 111 pmol/mg protein) (Fig. 7A). In addition, [$^{32}\text{S}_2$, ^{34}S]GSSSG was detected in plasma at a concentration of 25 ± 10 nM. The ratios of [^{32}S , ^{34}S]GSSH to [$^{32}\text{S}_2$]GSSH, [^{32}S , ^{34}S]CysSSH to [$^{32}\text{S}_2$]CysSSH, and [$^{32}\text{S}_2$, ^{34}S]CysSSSCys to [$^{32}\text{S}_3$]CysSSSCys in brain and spinal cord were 6.5 ± 2.8 , 10.6 [9.8–12.5], and 31.8 ± 9.8 respectively (Fig. 7B). These results show that GSSSG reaches different parts of the central nervous system, including the spinal cord, within 30 min after intranasal administration, and is converted to other sulfane sulfur species.

3.5. Intranasal administration of GSSSG increased sulfane sulfur levels in lumbar spinal cords after spinal cord ischemia

GSSSG protects the lumbar spinal cord from neurodegeneration 48 h after SCI. To investigate whether increased levels of sulfane sulfur in the lumbar spinal cord might contribute to the neuroprotective effect, we measured the change in sulfane sulfur levels 48 h after SCI. Compared to mice that underwent a sham operation, SCI followed by treatment with vehicle alone did not alter sulfane sulfur levels in the lumbar spinal cords (sham operation vs SCI followed by vehicle alone; 1.00 ± 0.30 vs 0.56 ± 0.13 ; $P = 0.0870$ by one-way ANOVA with Dunnett's multiple comparison test, Fig. 8A). In contrast, the levels of sulfane sulfur in the lumbar spinal cord in mice that underwent SCI and received intranasal administration of GSSSG were greater than those in mice that underwent SCI and received vehicle alone (SCI followed by GSSSG vs vehicle alone; 1.37 ± 0.50 vs 0.56 ± 0.13 ; $P = 0.0023$, Fig. 8A). These results suggest that the beneficial effects of GSSSG in preventing delayed paraplegia are associated with increased sulfane sulfur levels in lumbar spinal cords.

3.6. Effects of GSSSG on primary cortical neurons

To determine whether polysulfides increase sulfane sulfur levels

within neurons, we measured relative sulfane sulfur levels in primary cortical neurons using SSip-1 DA, in the presence and absence of polysulfides. SSip-1 DA is a fluorescent probe that can be used to measure the concentration of sulfane sulfur inside cells [38]. Relative to untreated primary cortical neurons, neurons that were incubated with GSSSG or Na_2S_3 had increased levels of intracellular sulfane sulfur (Fig. 8B).

In vivo studies showed that GSSSG can prevent neurodegeneration after SCI. To determine whether GSSSG can protect neurons from similar injury in vitro, primary cells were incubated with GSSSG after oxygen and glucose deprivation/reoxygenation (OGD/R). Cell viability was assessed using crystal violet and lactate dehydrogenase (LDH) assays, as previously described [39]. Crystal violet dye stains DNA and protein in cells and confirms that the cells are alive and able to maintain attachment to tissue culture plates despite OGD/R. The LDH assay measures the level of lactate dehydrogenase in tissue culture medium and is an indirect measure of plasma membrane damage. Compared to control cells, treatment with OGD/R was associated with a marked decrease in the number of live, adherent cells (Fig. 9A) and with a marked increase in the concentration of LDH in the tissue culture medium (Fig. 9B). Compared to vehicle-only treated cells, GSSSG at $30 \mu\text{M}$ increased cell viability as measured by the crystal violet assay (Fig. 9A), and GSSSG at $30 \mu\text{M}$ or $60 \mu\text{M}$ decreased release of LDH after OGD/R (Fig. 9B). A higher dose of GSSSG ($100 \mu\text{M}$) *per se* increased LDH levels in the tissue culture medium (Fig. S3) and failed to improve cell survival after OGD/R. These results show that GSSSG dose-dependently protects neurons from the effects of OGD/R.

In vivo studies showed that GSSSG, but not GSH or GSSG, prevents the development of delayed paraplegia after SCI, and suggested that the neuroprotective effects of GSSSG are derived from sulfane sulfur. To determine whether the neuroprotective effects of GSSSG on primary cultured neurons are derived from sulfane sulfur, we tested the ability of GSSSG, GSH, and GSSG to protect the neurons from OGD/R. Compared to vehicle-only treated cells, GSSSG at $30 \mu\text{M}$ improved cell viability after OGD/R (Fig. 9C). In contrast, GSH at $60 \mu\text{M}$ and GSSG at $30 \mu\text{M}$ did not improve cell viability after OGD/R (Fig. 9C). These results suggest that the neuroprotective effects of GSSSG are derived from sulfane sulfur.

3.7. Effects of PTN-SSS on SH-SY5Y cells

We used in vitro studies to show that GSSSG protects neurons after OGD/R, and to suggest that the neuroprotective effects of GSSSG are derived from sulfane sulfur. To investigate whether other polysulfides are cytoprotective after OGD/R, we examined the effect of PTN-SSS, another polysulfide, on the viability of SH-SY5Y cells after OGD/R. As

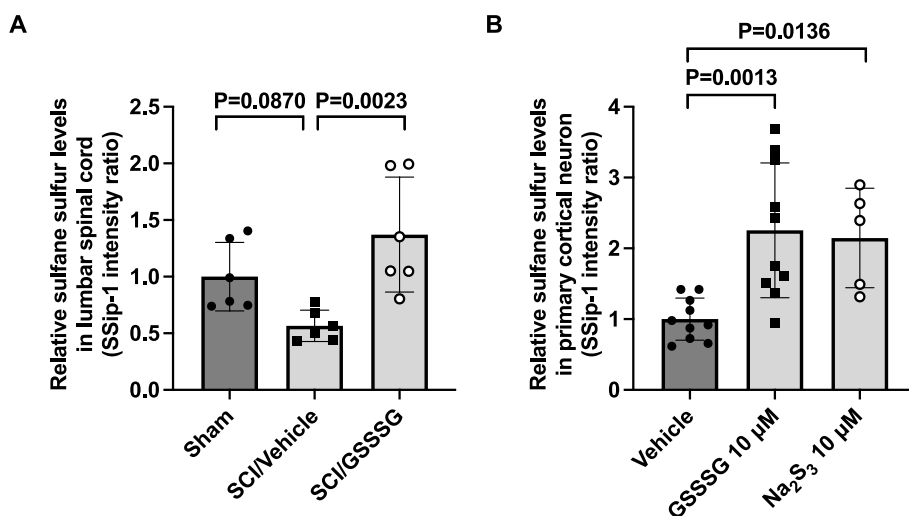


Fig. 8. GSSSG increased relative sulfane sulfur levels in lumbar spinal cord and primary cortical neurons. A. Relative sulfane sulfur levels in lumbar spinal cords at 48 h after surgery in mice subjected to a sham surgical procedure, or SCI and treated with GSSSG or vehicle alone. Relative sulfane sulfur levels in lumbar spinal cords were estimated using a fluorescent probe, SSip-1. $n = 6$ mice for each group. Data are presented as means with standard deviation. B. Relative sulfane sulfur levels in primary cortical neurons after incubation with GSSSG at $10 \mu\text{M}$, Na_2S_3 at $10 \mu\text{M}$, or vehicle alone. Data were analyzed using one-way ANOVA with Dunnett's multiple comparison test. $n = 10$ for GSSSG and vehicle groups. $n = 5$ for Na_2S_3 group. Data are presented as means with standard deviation.

Abbreviations: GSSSG, glutathione trisulfide; Na_2S_3 , sodium trisulfide; SCI, spinal cord ischemia.

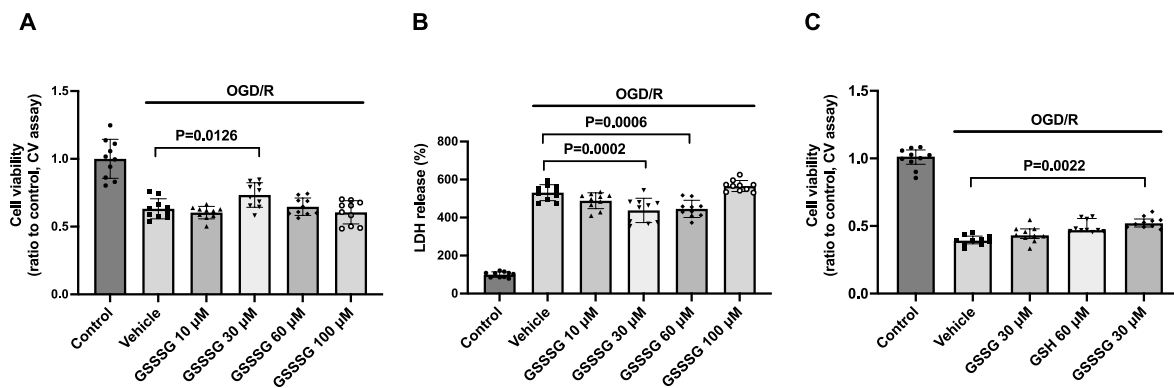


Fig. 9. GSSSG, but not GSH or GSSG, improved cell viability after oxygen and glucose deprivation/reoxygenation. A. Cell viability assessed by crystal violet assay after OGD/R when primary cortical neurons were incubated with GSSSG at various doses. Comparisons were made using one-way ANOVA with Dunnett's multiple comparison test. $n = 10$ for each group. Data are presented as means with standard deviation. B. Cell viability assessed by LDH assay after OGD/R when primary cortical neurons were incubated with GSSSG at various doses. Comparisons were made using one-way ANOVA with Dunnett's multiple comparison test. $n = 10$ for each group. Data are presented as means with standard deviation. C. The cell viability after OGD/R was assessed by crystal violet assay when primary cortical neurons were incubated with GSSSG at 30 μ M, GSH at 60 μ M, GSSG at 30 μ M, or vehicle alone. Comparisons were made using Kruskal-Wallis test with Dunn's multiple comparisons test. $n = 10$ for each group. Data are presented as medians with an interquartile range. Abbreviations: CV, crystal violet; GSH, glutathione; GSSG, glutathione disulfide; GSSSG, glutathione trisulfide; LDH, lactate dehydrogenase; OGD/R, oxygen and glucose deprivation/reoxygenation.

with primary cortical neurons, treatment with OGD/R reduced the viability of SH-SY5Y cells. Compared to vehicle-only treated cells, incubation with PTN-SSS at 10 μ M, 25 μ M, or 50 μ M significantly improved SH-SY5Y viability after OGD/R in a dose-dependent fashion (Fig. 10A). In contrast, PTN-SSS did not improve cell viability at 100 μ M because of a direct cytotoxic effect of PTN-SSS at high doses (Fig. S4). These results show that PTN-SSS dose-dependently rescues SH-SY5Y cells after OGD/R, and support that polysulfides are cytoprotective after OGD/R.

To determine whether the cytoprotective effects of PTN-SSS are relative to the amount of intracellular sulfane sulfur, we used SSip-1 DA to measure sulfane sulfur levels in SH-SY5Y cells after incubation with PTN-SSS. The level of sulfane sulfur inside SH-SY5Y cells increased with increasing concentration of PTN-SSS (Fig. 10B). The ability of SSip-1 DA (5 μ M) to measure intracellular sulfane sulfur reached a maximum with the concentration of PTN-SSS at 100 μ M (Fig. 10B). Compared to vehicle-only treated cells, the sulfane sulfur levels in SH-SY5Y cells increased significantly at the dose of PTN-SSS (10–50 μ M), which significantly improved cell viability after OGD/R. These results suggest that the cytoprotective effects of PTN-SSS are relative to the amount of sulfane sulfur released from PTN-SSS.

3.8. PTN-SSS increased the sulfane sulfur levels in the olfactory bulb and forebrain, and whole spinal cord shortly after intranasal administration

To study whether PTN-SSS increases sulfane sulfur levels in the central nervous system shortly after intranasal administration, we measured sulfane sulfur levels in the olfactory bulb and forebrain and the whole spinal cord 30 min after intranasal administration of PTN-SSS using SSip-1. Compared to mice that received intranasal administration of vehicle alone, intranasal administration of PTN-SSS increased sulfane sulfur levels in the olfactory bulb and forebrain and the whole spinal cord (Fig. 10C). These results suggest that PTN-SSS increases sulfane sulfur levels in the central nervous system within 30 min after intranasal administration.

3.9. Intranasal administration of PTN-SSS rescued mice from delayed paraplegia after transient spinal cord ischemia

In vitro studies showed that PTN-SSS is cytoprotective after OGD/R, and the cytoprotective effects of PTN-SSS are relative to the amount of sulfane sulfur released from PTN-SSS. As GSSSG prevented the

development of delayed paraplegia after SCI, and the neuroprotective effects of GSSSG were associated with sulfane sulfur, we hypothesized that PTN-SSS could also rescue mice from delayed paraplegia after SCI. In addition, as with GSSSG, we tested whether the sulfane sulfur in PTN-SSS, rather than PTN alone, was neuroprotective. Male mice received intranasal administration of PTN-SSS, PTN, or vehicle alone at 0, 8, 23, and 32 h after surgery. An equimolar dose of PTN-SSS (50 mg/kg) or PTN (47.3 mg/kg) was administered. Intranasal administration of PTN-SSS rescued 6 of 9 male mice (66%) from delayed paraplegia. In contrast, intranasal administration of PTN did not rescue any male mouse from delayed paraplegia. The BMS score at 72 h after surgery in the PTN-SSS group was significantly higher than that in the PTN or vehicle alone group (PTN-SSS vs PTN, BMS; 7.0 [1.5–9.0] vs 1.0 [0.0–2.0]; $P = 0.0323$. PTN-SSS vs vehicle alone, BMS; 7.0 [1.5–9.0] vs 1.0 [0.0–1.5]; $P = 0.0258$, Fig. 10D). These results show that PTN-SSS, but not PTN, prevents the development of delayed paraplegia after SCI in mice, indicating that the neuroprotective effects of PTN-SSS are derived from sulfane sulfur, not PTN.

4. Discussion

In this study, we show that the post-reperfusion intranasal administration of GSSSG, but not GSH or GSSG, prevented the extensive loss of viable neurons in the ventral horns of the lumbar spinal cord and rescued mice from delayed paraplegia after SCI. In primary cortical neurons, GSSSG, but not GSH or GSSG, improved cell viability after OGD/R. The beneficial effects of GSSSG were associated with inhibition of increased levels of inflammatory cytokines and inhibition of microglial- and caspase-3 activation. A marked increase in several 34 S-labeled sulfane sulfur species was detected in the lumbar spinal cord shortly after intranasal administration of GSSSG. Furthermore, we observed that the protective effects of GSSSG were associated with increased sulfane sulfur levels in the lumbar spinal cord after intranasal administration of GSSSG and in primary cortical neurons after incubation with GSSSG. In addition, incubation of SH-SY5Y cells with PTN-SSS increased intracellular sulfane sulfur levels and improved cell viability after OGD/R, and the post-reperfusion intranasal administration of PTN-SSS, but not PTN, rescued mice from delayed paraplegia after SCI. PTN-SSS increased sulfane sulfur levels in the central nervous system shortly after intranasal administration. These observations suggest that sulfane sulfur can be readily delivered to the central nervous system with intranasal administration of polysulfides and that this treatment

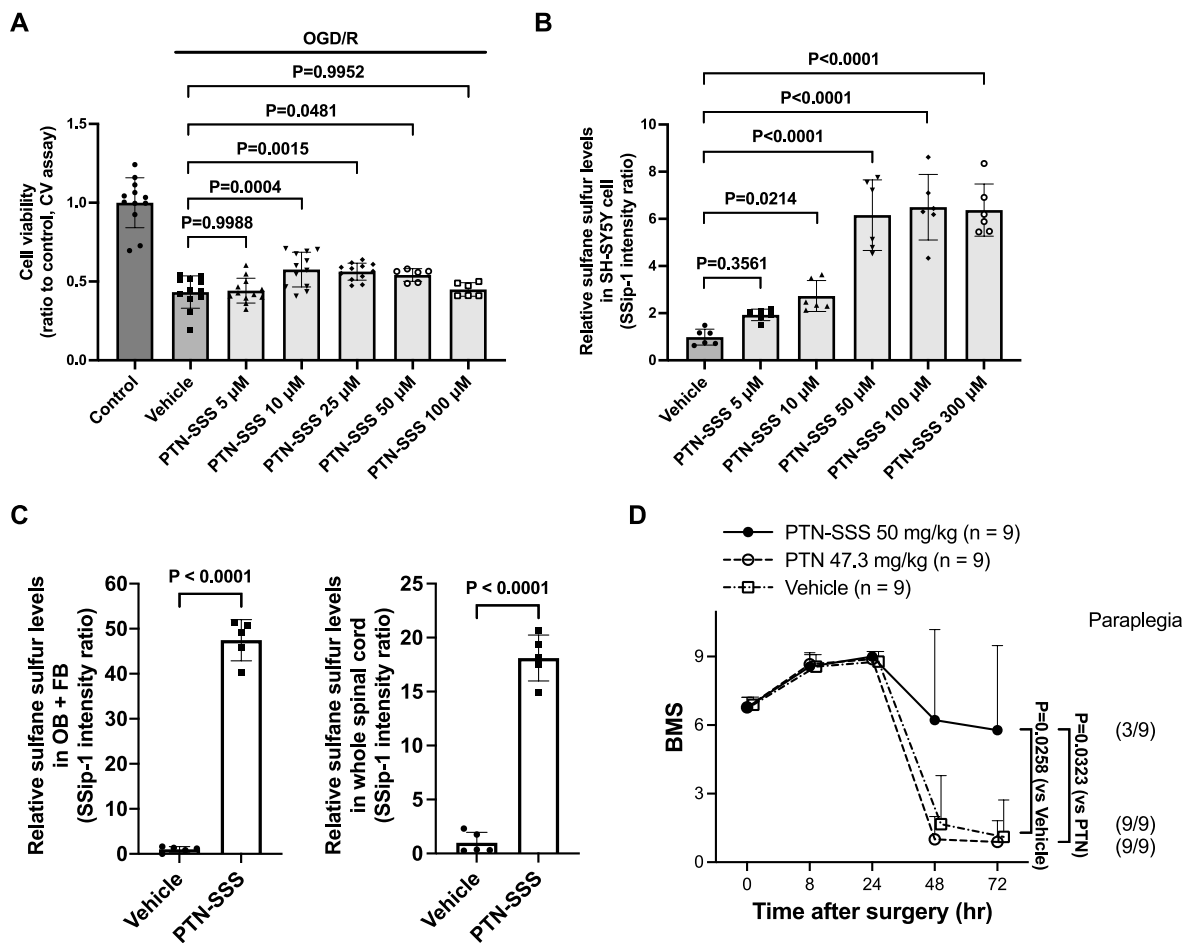


Fig. 10. PTN-SSS improved cell viability after OGD/R and prevented delayed paraplegia after SCI as a post-reperfusion treatment. A. Cell viability was assessed using the crystal violet assay after OGD/R when SH-SY5Y cells were incubated with PTN-SSS at 5 μ M, 10 μ M, 25 μ M, 50 μ M, 100 μ M, or vehicle alone. Comparisons were made using one-way ANOVA with Dunnett's multiple comparison test. $n = 12$ for control, vehicle alone and PTN-SSS at 5 μ M, 10 μ M, and 25 μ M $n = 6$ for PTN-SSS at 50 μ M and 100 μ M. Data are presented as means with standard deviation. B. Relative sulfane sulfur levels in SH-SY5Y cells after incubation with PTN-SSS at 5 μ M, 10 μ M, 50 μ M, 100 μ M, 300 μ M, or vehicle alone. Comparisons were made using one-way ANOVA with Dunnett's multiple comparison test. $n = 6$ for each group. Data are presented as means with standard deviation. C. Relative sulfane sulfur levels in the olfactory bulb and forebrain and the whole spinal cord at 30 min after intranasal administration of PTN-SSS. Relative sulfane sulfur levels were estimated using a fluorescent probe, SSip-1. Comparisons were made using unpaired *t*-test. $n = 5$ mice for each group. Data are presented as means with standard deviation. D. Changes of the BMS scores for 72 h after SCI in male mice subjected to SCI and treated with vehicle alone, PTN, or PTN-SSS. Comparisons were made using the Kruskal-Wallis test with Dunn's multiple comparisons test. $n = 9$ mice for each group. Data are presented as means with standard deviation.

Abbreviations: BMS, Basso mouse scale for locomotion; CV, crystal violet; LDH, lactate dehydrogenase; OB + FB, olfactory bulb and forebrain; OGD/R, oxygen and glucose deprivation/reoxygenation; PTN, pantethine; PTN-SSS, pantethine trisulfide; SCI, spinal cord ischemia.

prevents delayed neurodegeneration in the lumbar spinal cord, mitigating delayed paraplegia. The results of this study underscore the important therapeutic potential of polysulfides in preventing neurodegeneration of the spinal cord.

Previously, we used a chemically-induced cytotoxicity model using SH-SY5Y cells to show that the cytoprotective effects of H₂S-donor compounds were correlated with their ability to increase intracellular sulfane sulfur levels [45]. We also reported that the administration of sodium thiosulfate improved the survival and neurological function of mice subjected to global cerebral ischemia-reperfusion; the cytoprotective effects were associated with a marked increase in thiosulfate (a sulfane sulfur species) in plasma and brain tissues [46]. These results suggest that increasing the concentration of sulfane sulfur may be neuroprotective in pathological conditions. In this study, we showed that the neuroprotective effects of intranasal GSSSG in SCI-induced spinal cord injury were associated with increased sulfane sulfur levels in lumbar spinal cords. The results support the hypothesis that the neuroprotective effects of GSSSG are mediated by increased sulfane sulfur.

Previous preclinical studies suggested that administration of GSH

ameliorates neuronal cell death after brain ischemia-reperfusion [21, 47]. Because GSH is a metabolic product of GSSSG [9,17], it was possible that an increased concentration of GSH could explain the neuroprotective effects of GSSSG. However, in the current study, we observed that intranasal administration of GSSSG, but not GSH, prevented delayed paraplegia after SCI. The reason for the discrepancy between the current and previous reports regarding the effects of GSH might arise from differences in doses of GSH, routes of administration, and animal models. In particular, the dose of GSH used in the current study was one-tenth of that used in previous studies. The results of this study support the hypothesis that the mechanism of GSSSG-mediated neuroprotection is independent of conversion to GSH.

Intracellular sulfane sulfur species can react with GSH, resulting in the generation of GSSH [9]. Compared with GSH, GSSH is more nucleophilic and is a better intracellular antioxidant. In addition, GSSH can be directly generated from GSSSG [9]. Akaike and colleagues reported that the concentration of endogenous GSSH in the brain of mice is 222 pmol/mg protein, which is significantly greater than that of other endogenous sulfane sulfur species, including GSSSG (1 pmol/mg

protein), CysSSH (2 pmol/mg protein), or CysSSSCys (not detected) [9, 37]. In the current study, ^{34}S -labeled GSSSG was detected at 317 ± 111 pmol/mg protein in the lumbar spinal cord 30 min after intranasal administration of GS^{34}SSG . Furthermore, based on the previously reported levels of endogenous GSSH and CysSSH [37], the levels of ^{34}S -labeled GSSH and ^{34}S -labeled CysSSH in lumbar spinal cord after intranasal administration of GS^{34}SSG would have been approximately 1600 pmol/mg protein and 18 pmol/mg protein, respectively [9,37]. These results show that intranasal administration of GSSSG can increase the levels of multiple sulfane sulfur species by about 10 to 100-fold in the lumbar spinal cord, the epicenter of neuronal death after SCI. Considering that GSSH is quantitatively the most predominant sulfane sulfur species in lumbar spinal cord after intranasal administration of GSSSG, the bulk of neuroprotective effect of GSSSG might be conferred via GSSH.

Previous studies showed that, after systemic administration, molecules larger than 500 Da were unable to pass through the blood-brain barrier and blood-spinal cord barrier [31]. Because of the large size of GSSSG (644.7 Da), we chose to administer this compound intranasally. After intranasal administration, large molecules can bypass blood-brain and blood-spinal cord-barriers through the olfactory and trigeminal neural pathways, and can rapidly reach the parenchyma of the central nervous system [30,32]. The peripheral olfactory system connects the nasal passages with the olfactory bulbs and rostral brain, and the peripheral trigeminal system connects the nasal passages with the brainstem and spinal cord [30]. For example, a previous report compared the intravenous and intranasal routes of administration on the amount of methylprednisolone sodium succinate (497.5 Da) that reached the spinal cord [48]. While a relatively large amount of methylprednisolone was detected in the parenchyma of the spinal cord after intranasal administration, a much smaller amount of methylprednisolone was detected after intravenous administration [48]. Various other high molecular weight-therapeutics (>500 Da) were successfully delivered to the central nervous system by intranasal administration [49]. In the current study, we observed that the concentration of ^{34}S -labeled GSSSG in the central nervous system (268 ± 140 pmol/mg protein) was markedly higher than that of endogenous GSSSG in the brains of mice (1 pmol/mg protein) [37] at 30 min after intranasal administration of GS^{34}SSG . In contrast, the concentration of ^{34}S -labeled GSSSG in plasma (25 ± 10 nM) was significantly lower than endogenous GSSSG in the plasma of wild-type mice (125 nM, unpublished data by Akaike and colleagues). These results suggest that intranasally-administered GSSSG readily and preferentially reaches the central nervous system, including the spinal cord, through the olfactory and trigeminal neural pathways, rather than the blood stream.

There are some limitations to this study. First, we did not determine the detailed mechanism responsible for the beneficial effects of polysulfides beyond the fact that the effects are associated with increased levels of sulfane sulfur in the target organ, inhibition of increased levels of inflammatory cytokines, and inhibition of microglial- and caspase-3-activation, and are unlikely to be attributable to transglutathionylation. Polysulfides appear to be cytoprotective via multiple mechanisms including acting as antioxidants [9,10] and anti-inflammatory agents [10,11], inhibiting lipid peroxidation and ferroptosis [12], and enhancing post-translational modifications of proteins [13,14]. The precise mechanisms responsible for the neuroprotective effects of polysulfides remain to be elucidated in future studies. Second, we did not investigate the mechanism by which GSSSG suppressed the mRNA level of SQOR, a protein that catabolizes sulfides to GSSH. The increased level of GSSH after intranasal administration of GSSSG might downregulate expression of SQOR via negative feedback. Third, although GSSSG and PTN-SSS were administered intranasally under mild sedation, some mice expectorated the drugs from their noses or swallowed them. It is likely that the cytoprotective effects conferred by polysulfides in this study reflect the effects of a lower dose being successfully administered. As better drug formulations, which are more suitable for clinical

application, are developed, we anticipate that the beneficial effects of polysulfides will be achieved using lower doses.

In conclusion, the current study revealed that the post-reperfusion intranasal administration of GSSSG or PTN-SSS, but not GSH, GSSG, or PTN, rescues mice subjected to SCI from delayed paraplegia. Intranasally-administered GSSSG accumulated in the lumbar spinal cord, increased the local concentrations of persulfides, polysulfides, and sulfane sulfur, and decreased neuroinflammation, apoptosis, and neurodegeneration. The potent neuroprotective effect of intranasally-administered GSSSG is similar to that of inhaled H_2S , but the use of polysulfides, including GSSSG and PTN-SSS, is far more practical in clinical medicine than administration of gaseous H_2S . In particular, the excellent physical properties of PTN-SSS warrants further evaluation for clinical development. This study opens up the possibility of a novel polysulfide-based therapy to prevent the development of delayed paraplegia after thoracoabdominal aortic surgery and other neurodegenerative diseases of the spinal cord.

Funding statement

This study was supported by a sponsored research agreement from Kyowa Hakko Bio Co., Ltd. (Tokyo, Japan) to FI, and funds from Luisa Hunnewell and Larry Newman (Wellesley, MA) and The Feil Family Foundation (NY, NY) to DBB.

Declaration of competing interest

The authors declare the following financial interests/personal relationships which may be considered as potential competing interests: FI receives research funding from Kyowa-Hakko Bio. EK, ME, EM, EO and FI are listed as inventors of patents filed by MGH related to GSSSG and PTN-SSS. EO is an employee of Kyowa Hakko Bio.

Data availability

Data will be made available on request.

Acknowledgments

GSSSG, ^{34}S -labeled GSSSG, GSSG, and PTN-SSS were provided by Kyowa Hakko Bio Co., Ltd. (Tokyo, Japan). SSip-1 and SSip-1-DA were kindly provided by Dr. Kenjiro Hanaoka (Graduate School of Pharmaceutical Sciences, Keio University, Tokyo, Japan). HPE-IAM LC-MS/MS sulfide metabolite analysis was performed by the Center for Redox Biology and Cardiovascular Disease at LSU Health Shreveport (Shreveport, LA) supported by an Institutional Development Award (IDeA) from the National Institutes of General Medical Sciences of the NIH (Bethesda, MD) under grant number GM121307. Authors thank Dr. Takaaki Akaike (Department of Environmental Medicine and Molecular Toxicology, Tohoku University School of Medicine, Sendai, Japan) for sharing unpublished data on the plasma levels of GSSSG in mice.

Appendix A. Supplementary data

Supplementary data to this article can be found online at <https://doi.org/10.1016/j.redox.2023.102620>.

References

- [1] B.A. Ziganshin, J.A. Elefteriades, Surgical management of thoracoabdominal aneurysms, *Heart* 100 (2014) 1577–1582.
- [2] V. Riambau, D. Böckler, J. Brunkwall, P. Cao, R. Chiesa, G. Coppi, M. Czerny, G. Fraedrich, S. Haulon, M.J. Jacobs, M.L. Lachat, F.L. Moll, C. Setacci, P.R. Taylor, M. Thompson, S. Trimarchi, H.J. Verhagen, E.L. Verhoeven, C. Esvs Guidelines, P. Kolh, G.J. de Borst, N. Chakfé, E.S. Debus, R.J. Hinchliffe, S. Kakkos, I. Koncar, J. S. Lindholt, M. Vega de Ceniga, F. Vermassen, F. Verzini, R. Document, P. Kolh, J. H. Black 3rd, R. Busund, M. Björck, M. Dake, F. Dick, H. Eggebrecht, A. Evangelista, M. Grabenwöger, R. Milner, A.R. Naylor, J.B. Ricco, H. Rousseau,

- J. Schmidli, Editor's choice - management of descending thoracic aorta diseases: clinical practice guidelines of the European society for vascular surgery (ESVS), *Eur. J. Vasc. Endovasc. Surg.* 53 (2017) 4–52.
- [3] C.D. Etz, M. Luehr, F.A. Kari, C.A. Bodian, D. Smego, K.A. Plestis, R.B. Griep, Paraplegia after extensive thoracic and thoracoabdominal aortic aneurysm repair: does critical spinal cord ischemia occur postoperatively? *J. Thorac. Cardiovasc. Surg.* 135 (2008) 324–330.
- [4] B.W. Ullery, A.T. Cheung, R.M. Fairman, B.M. Jackson, E.Y. Woo, J. Bavaria, A. Pochettino, G.J. Wang, Risk factors, outcomes, and clinical manifestations of spinal cord ischemia following thoracic endovascular aortic repair, *J. Vasc. Surg.* 54 (2011) 677–684.
- [5] J.F. Wang, Y. Li, J.N. Song, H.G. Pang, Role of hydrogen sulfide in secondary neuronal injury, *Neurochem. Int.* 64 (2014) 37–47.
- [6] M. Kakinohana, K. Kida, S. Minamishima, D.N. Atochin, P.L. Huang, M. Kaneki, F. Ichinose, Delayed paraplegia after spinal cord ischemic injury requires caspase-3 activation in mice, *Stroke* 42 (2011) 2302–2307.
- [7] J.L. Wallace, R. Wang, Hydrogen sulfide-based therapeutics: exploiting a unique but ubiquitous gasotransmitter, *Nat. Rev. Drug Discov.* 14 (2015) 329–345.
- [8] H. Kimura, Signalling by hydrogen sulfide and polysulfides via protein S-sulfuration, *Br. J. Pharmacol.* 177 (2020) 720–733.
- [9] T. Ida, T. Sawa, H. Ihara, Y. Tsuchiya, Y. Watanabe, Y. Kumagai, M. Suematsu, H. Motohashi, S. Fujii, T. Matsunaga, M. Yamamoto, K. Ono, N.O. Devarie-Baez, M. Xian, J.M. Fukuto, T. Akaike, Reactive cysteine persulfides and S-polythiolation regulate oxidative stress and redox signaling, *Proc. Natl. Acad. Sci. U. S. A.* 111 (2014) 7606–7611.
- [10] T. Sawa, H. Motohashi, H. Ihara, T. Akaike, Enzymatic regulation and biological functions of reactive cysteine persulfides and polysulfides, *Biomolecules* 10 (2020) 1245.
- [11] T. Zhang, K. Ono, H. Tsutsuki, H. Ihara, W. Islam, T. Akaike, T. Sawa, Enhanced cellular polysulfides negatively regulate TLR4 signaling and mitigate lethal endotoxin shock, *Cell. Chem. Biol.* 26 (2019), 686–98.e4.
- [12] U. Barayeu, D. Schilling, M. Eid, T.N. Xavier da Silva, L. Schlicker, N. Mitreska, C. Zapp, F. Gräter, A.K. Miller, R. Kappl, A. Schulze, J.P. Friedmann Angeli, T. P. Dick, Hydropersulfides inhibit lipid peroxidation and ferroptosis by scavenging radicals, *Nat. Chem. Biol.* (2022), <https://doi.org/10.1038/s41589-022-01145-w>.
- [13] H. Kimura, Signaling molecules: hydrogen sulfide and polysulfide, *Antioxidants Redox Signal.* 22 (2015) 362–376.
- [14] I. Braunstein, R. Engelman, O. Yitzhaki, T. Ziv, E. Galardon, M. Benhar, Opposing effects of polysulfides and thioredoxin on apoptosis through caspase persulfidation, *J. Biol. Chem.* 295 (2020) 3590–3600.
- [15] M. Kakinohana, E. Marutani, K. Tokuda, K. Kida, S. Kosugi, S. Kasamatsu, A. Magliocca, K. Ikeda, S. Kai, M. Sakaguchi, S. Hirai, M. Xian, M. Kaneki, F. Ichinose, Breathing hydrogen sulfide prevents delayed paraplegia in mice, *Free Radic. Biol. Med.* 131 (2019) 243–250.
- [16] E.A. Wintner, T.L. Deckwerth, W. Langston, A. Bengtsson, D. Leviten, P. Hill, M. A. Insko, R. Dumpit, E. VandenEckart, C.F. Toombs, C. Szabo, A monobromobimane-based assay to measure the pharmacokinetic profile of reactive sulphide species in blood, *Br. J. Pharmacol.* 160 (2010) 941–957.
- [17] C.L. Bianco, T. Akaike, T. Ida, P. Nagy, V. Bogdandi, J.P. Toscano, Y. Kumagai, C. F. Henderson, R.N. Goddu, J. Lin, J.M. Fukuto, The reaction of hydrogen sulfide with disulfides: formation of a stable trisulfide and implications for biological systems, *Br. J. Pharmacol.* 176 (2019) 671–683.
- [18] H. Kunikata, T. Ida, K. Sato, N. Aizawa, T. Sawa, H. Tawarayama, N. Murayama, S. Fujii, T. Akaike, T. Nakazawa, Metabolomic profiling of reactive persulfides and polysulfides in the aqueous and vitreous humors, *Sci. Rep.* 7 (2017), 41984.
- [19] T. Numakura, H. Sugiura, T. Akaike, T. Ida, S. Fujii, A. Koorai, M. Yamada, K. Onodera, Y. Hashimoto, R. Tanaka, K. Sato, Y. Shishikura, T. Hirano, S. Yanagisawa, N. Fujino, T. Okazaki, T. Tamada, Y. Hoshikawa, Y. Okada, M. Ichinose, Production of reactive persulfide species in chronic obstructive pulmonary disease, *Thorax* 72 (2017) 1074–1083.
- [20] K. Aquilano, S. Baldelli, M.R. Ciriolo, Glutathione: new roles in redox signaling for an old antioxidant, *Front. Pharmacol.* 5 (2014) 196.
- [21] Y. Yabuki, K. Fukunaga, Oral administration of glutathione improves memory deficits following transient brain ischemia by reducing brain oxidative stress, *Neuroscience* 250 (2013) 394–407.
- [22] S.S. Sadhu, J. Xie, H. Zhang, O. Perumal, X. Guan, Glutathione disulfide liposomes - a research tool for the study of glutathione disulfide associated functions and dysfunctions, *Biochem. Biophys. Rep.* 7 (2016) 225–229.
- [23] D. Giustarini, R. Rossi, A. Milzani, R. Colombo, I. Dalle-Donne, S-glutathionylation, From redox regulation of protein functions to human diseases, *J. Cell Mol. Med.* 8 (2004) 201–212.
- [24] Y. Xiong, J.D. Uys, K.D. Tew, D.M. Townsend, S-glutathionylation, From molecular mechanisms to health outcomes, *Antioxidants Redox Signal.* 15 (2011) 233–270.
- [25] F. Tóth, E.K. Cseh, L. Vécsei, Natural molecules and neuroprotection: kynurenic acid, pantethine and α -lipoic acid, *Int. J. Mol. Sci.* 22 (2021) 403.
- [26] D. Brunetti, S. Dusi, C. Giordano, C. Lamperti, M. Morbin, V. Fuganesi, S. Marchet, G. Fagioliari, O. Sibon, M. Moggio, G. d'Amati, V. Tiranti, Pantethine treatment is effective in recovering the disease phenotype induced by ketogenic diet in a pantothenate kinase-associated neurodegeneration mouse model, *Brain* 137 (2014) 57–68.
- [27] K. Baranger, M. van Gijssel-Bonnelo, D. Stephan, W. Carpentier, S. Rivera, M. Khrestchatsky, B. Gharib, M. De Reggi, P. Benech, Long-term pantethine treatment counteracts pathologic gene dysregulation and decreases alzheimer's disease pathogenesis in a transgenic mouse model, *Neurotherapeutics* 16 (2019) 1237–1254.
- [28] P.D. Smith, F. Puskas, X. Meng, D. Cho, J.C. Cleveland Jr., M.J. Weyant, M. T. Watkins, D.A. Fullerton, T.B. Reece, Ischemic dose-response in the spinal cord: both immediate and delayed paraplegia, *J. Surg. Res.* 174 (2012) 238–244.
- [29] P.D. Smith, F. Puskas, X. Meng, J.H. Lee, J.C. Cleveland Jr., M.J. Weyant, D. A. Fullerton, T.B. Reece, The evolution of chemokine release supports a bimodal mechanism of spinal cord ischemia and reperfusion injury, *Circulation* 126 (2012) S110–S117.
- [30] R.G. Thorne, G.J. Pronk, V. Padmanabhan, W.H. Frey 2nd, Delivery of insulin-like growth factor-I to the rat brain and spinal cord along olfactory and trigeminal pathways following intranasal administration, *Neuroscience* 127 (2004) 481–496.
- [31] F. Rossi, G. Perale, S. Papa, G. Forloni, P. Veglianesi, Current options for drug delivery to the spinal cord, *Exp. Opin. Drug Deliv.* 10 (2013) 385–396.
- [32] V. Bartanusz, D. Jezova, B. Alajajian, M. Digiçaylioglu, The blood-spinal cord barrier: morphology and clinical implications, *Ann. Neurol.* 70 (2011) 194–206.
- [33] H. Awad, D.P. Ankeny, Z. Guan, P. Wei, D.M. McTigue, P.G. Popovich, A mouse model of ischemic spinal cord injury with delayed paralysis caused by aortic cross-clamping, *Anesthesiology* 113 (2010) 880–891.
- [34] D.M. Basso, L.C. Fisher, A.J. Anderson, L.B. Jakeman, D.M. McTigue, P. G. Popovich, Basso Mouse Scale for locomotion detects differences in recovery after spinal cord injury in five common mouse strains, *J. Neurotrauma* 23 (2006) 635–659.
- [35] T. Takata, M. Jung, T. Matsunaga, T. Ida, M. Morita, H. Motohashi, X. Shen, C. G. Kevil, J.M. Fukuto, T. Akaike, Methods in sulfide and persulfide research, *Nitric Oxide* 116 (2021) 47–64.
- [36] H.A. Hamid, A. Tanaka, T. Ida, A. Nishimura, T. Matsunaga, S. Fujii, M. Morita, T. Sawa, J.M. Fukuto, P. Nagy, R. Tsutsumi, H. Motohashi, H. Ihara, T. Akaike, Polysulfide stabilization by tyrosine and hydroxyphenyl-containing derivatives that is important for a reactive sulfur metabolomics analysis, *Redox Biol.* 21 (2019), 101096.
- [37] S. Kasamatsu, T. Ida, T. Koga, K. Asada, H. Motohashi, H. Ihara, T. Akaike, High-precision sulfur metabolomics innovated by a new specific probe for trapping reactive sulfur species, *Antioxidants Redox Signal.* 34 (2021) 1407–1419.
- [38] Y. Takano, K. Hanaoka, K. Shimamoto, R. Miyamoto, T. Komatsu, T. Ueno, T. Terai, H. Kimura, T. Nagano, Y. Urano, Development of a reversible fluorescent probe for reactive sulfur species, sulfane sulfur, and its biological application, *Chem. Commun.* 53 (2017) 1064–1067.
- [39] E. Marutani, S. Kosugi, K. Tokuda, A. Khatri, R. Nguyen, D.N. Atochin, K. Kida, K. Van Leyen, K. Arai, F. Ichinose, A novel hydrogen sulfide-releasing N-methyl-D-aspartate receptor antagonist prevents ischemic neuronal death, *J. Biol. Chem.* 287 (2012) 32124–32135.
- [40] F. Faul, E. Erdfelder, A.G. Lang, A. Buchner, G*Power 3: a flexible statistical power analysis program for the social, behavioral, and biomedical sciences, *Behav. Res. Methods* 39 (2007) 175–191.
- [41] C.H. Switzer, S. Guttzeit, T.R. Eykyn, P. Eaton, Cysteine trisulfide oxidizes protein thiols and induces electrophilic stress in human cells, *Redox Biol.* 47 (2021), 102155.
- [42] Y. Gao, R. Fu, J. Wang, X. Yang, L. Wen, J. Feng, Resveratrol mitigates the oxidative stress mediated by hypoxic-ischemic brain injury in neonatal rats via Nrf2/HO-1 pathway, *Pharm. Biol.* 56 (2018) 440–449.
- [43] M.T. Bell, F. Puskas, V.A. Agoston, J.C. Cleveland Jr., K.A. Freeman, F. Gamboni, P. S. Herson, X. Meng, P.D. Smith, M.J. Weyant, D.A. Fullerton, T.B. Reece, Toll-like receptor 4-dependent microglial activation mediates spinal cord ischemia-reperfusion injury, *Circulation* 128 (2013) S152–S156.
- [44] D. Ito, K. Tanaka, S. Suzuki, T. Dembo, Y. Fukuuchi, Enhanced expression of Iba1, ionized calcium-binding adapter molecule 1, after transient focal cerebral ischemia in rat brain, *Stroke* 32 (2001) 1208–1215.
- [45] E. Marutani, M. Sakaguchi, W. Chen, K. Sasakura, J. Liu, M. Xian, K. Hanaoka, T. Nagano, F. Ichinose, Cytoprotective effects of hydrogen sulfide-releasing N-methyl-D-aspartate receptor antagonists are mediated by intracellular sulfane sulfur, *Medchemcomm* 5 (2014) 1577–1583.
- [46] E. Marutani, M. Yamada, T. Ida, K. Tokuda, K. Ikeda, S. Kai, K. Shirozu, K. Hayashida, S. Kosugi, K. Hanaoka, M. Kaneki, T. Akaike, F. Ichinose, Thiosulfate mediates cytoprotective effects of hydrogen sulfide against neuronal ischemia, *J. Am. Heart Assoc.* 4 (2015), e002125.
- [47] J. Song, J. Park, Y. Oh, J.E. Lee, Glutathione suppresses cerebral infarct volume and cell death after ischemic injury: involvement of FOXO3 inactivation and Bcl2 expression, *Oxid. Med. Cell. Longev.* 2015 (2015), 426069.
- [48] D. Rassy, B. Bárcena, I.N. Pérez-Osorio, A. Espinosa, A.N. Peón, L.I. Terrazas, G. Meneses, H.O. Besedovsky, G. Fragoso, E. Scituito, Intranasal methylprednisolone effectively reduces neuroinflammation in mice with experimental autoimmune encephalitis, *J. Neuropathol. Exp. Neurol.* 79 (2020) 226–237.
- [49] L.R. Hanson, W.H. Frey 2nd, Intranasal delivery bypasses the blood-brain barrier to target therapeutic agents to the central nervous system and treat neurodegenerative disease, *BMC Neurosci.* 9 (Suppl 3) (2008) S5.